Journal of Applied Fluid Mechanics, Vol. 11, No. 1, pp. 177-189, 2018.
Available online at www.jafmonline.net, ISSN 1735-3572, EISSN 1735-3645.
DOI: 10.29252/jafm.11.01.28080

Mixed Convection Heat Transfer of Al_2O_3 Nanofluid on the Elliptical Shapes: Numerical Study of Irreversibility

K. Khajeh, L. Jahanshaloo, S. Ebrahimi and H. Aminfar†

Faculty of Mechanical Engineering, University of Tabriz, Tabriz, Iran

†*Corresponding Author Email: hh_aminfar@tabrizu.ac.ir*

(Received June 4, 2017; accepted September 17, 2017)

ABSTRACT

In this study the 2D laminar and steady water-based Al_2O_3 nanofluid flow over a cylinder with circular, horizontal and vertical elliptical cross section by constant surface temperature boundary condition has been studied. The main goal of this research is to investigate the effects of different natural and mixed convection heat transfer mechanisms on the convective heat transfer coefficient, and the entropy generation due to the thermal and frictional origination. Conservation equations of the mass, momentum and energy under the assumption of incompressible, Newtonian nanofluid, by using the homogeneous single phase method have been solved. The impact of considered parameters in this study (alteration in cross section, convective flow direction and volume fraction of nano particles) in enhancing the heat transfer rate is studied in association with the entropy generated value in each case. Based on the results, the vertical elliptical cross section, in comparison with others, shows the highest entropy generation value and the heat transfer coefficient in all considered mechanisms. Moreover, mixed convection heat transfer type 2, in which the force flow is perpendicular to the buoyant flow direction, has the highest entropy generation and heat transfer rate for all cross sections. In addition, in all cases in the presence of the nanoparticles, the heat transfer rate and entropy generation increases.

Keywords: Mixed convection; Nanofluid; Homogeneous single phase; Elliptic cylinder; Entropy generation.

NOMENCLATURE

a	major axis of the ellipse and circle diameter
b	minor axis of the ellipse
C_p	heat capacity
g	gravity acceleration
Gr	Grashof Number
h	average heat transfer coefficient
k	heat transfer conductivity coefficient
Nu	Nusselt number
$\dot{S}_{gen,\Delta T}$	the heat entropy generation
$\dot{S}_{gen,\Delta P}$	the friction entropy generation
p	pressure
P	dimensionless pressure
Pr	Prandtl Number
$\bar{q}$	the average surface heat flux
Ra	Rayleigh number
Re	Reynolds number
Ri	Richardson number
T	temperature
u, v	velocity components
U, V	dimensionless velocity components
x, y	cartesian coordinates
X, Y	dimensionless Cartesian coordinates

Greek symbols

α	thermal diffusivity
β	thermal expansion coefficient
θ	nondimensional temperature
μ	dynamic
ν	Kinematic Viscosity
ρ	density
Φ	volume fraction

Indices

f	base fluid
nf	vanofluid
p	vanoparticle
S	cylinder surface
∞	inlet characteristics

1. INTRODUCTION

The natural and mixed convection heat transfer around the bluff bodies have been studied by many researchers owing to their wide application in engineering. Designing the heat exchangers, cooling towers, high voltage power plants, photovoltaic thermal hybrid solar collectors, electrical devices, nucleate safety systems and food processing plants are of the examples of such applications. The numerical results of laminar and transitional flow for a wide range of Rayleigh numbers portrayed the effectiveness and the importance of different approaches to study the thermo-physical properties, structure, characteristics and configuration of the flow in these problems (Krishne Gowda, Aswatha Narayana *et al*. 1996, Corcione and Habib 2009, Kang and Chung 2012, Dawood, Mohammed *et al*. 2015, Garoosi, Jahanshaloo *et al*. 2015).

Since the early 1970s studying the free convection of flow past the horizontal cylinder with non-circular cross section has been highlighted as a research topic. In this matter, the elliptical cross section, due to its inclusion of a wide range of geometries from the flat plate to circular cylinders, draws the greatest interest (Merkin 1977, Terukazu, Hideya *et al*. 1984, Badr 1994).

Shin and Chang (1989) have been studied the transient free convection of the water and air flows from a horizontal circular cylinder which was subjected to a sudden temperature variation of the Rayleigh number ranged $10^3 < Ra < 10^6$. The results showed an increase in average Nusselt number by increasing the Rayleigh number in steady and unsteady flow simulation for both cases. Lin and Chao (1976) have performed the earliest study of free convection boundary layer over the 2D and axisymmetric isothermal smooth objects with fairly arbitrary shape. They examined a number of body configuration of aspect ratios ranged between 0.25 to 1 and flow properties of Prandtl number from 0.79 to ∞ for the horizontal and vertical cylinder. For the circular cylinder and the slender ellipses the local Nusselt number achieves a maximum at the stagnation point and reduces along the ellipse due to the boundary layer thickness variation. However, for blunt ellipses the local heat transfer coefficient and the local Nusselt number at first increases with distance from the stagnation point and reaches a maximum at the location which corresponds to an eccentric angle of approximately 86 degrees and then decreases to the rear half of the ellipse. The first experimental study of free convection heat transfer of air flow over an axisymmetric elliptical body have been done by Huang and Mayinger (1984). The local and average heat transfer coefficients for various slenderness ratios of the elliptical cross-section (0.364 to 0.667) and a range of Grashof number (4.5×10^4 to 3.77×10^5), in different configuration from horizontal to vertical cylinder have been measured. The obtained results indicated that the orientation of the major axis of the ellipse from horizontal to vertical inclination is associated with the increase of the average Nusselt number. They established an equation for the average heat transfer coefficient of elliptical cylinders, in which a geometrical coefficient takes into account the aspect ratio of the ellipse. The steady laminar free convection from a horizontal elliptic cylinder considering uniform surface temperature has been simulated by Corcione and Habib (2009). The study has been performed for the minor and major axis ratios of the elliptical cross-section of the cylinder in the range between 0.05 and 0.98 and inclination angles of the major axis of the ellipse with respect to gravity changed from 0° to 90°. Furthermore, the Rayleigh numbers supposed to be in the range between 10 and 10^7, and Prandtl numbers varied between 0.7 and 700. According to the results of study, the average Nusselt number increases with the Rayleigh and Prandtl numbers enhancement. At the same time, the heat transfer rate decreases with increasing the orientation angle of the cross-section of the cylinder or, in a simple word, passing from the slender to the blunt configuration.

One of the most important interests in free convection from a cylinder is the limitation of heat transfer rate. This drawback could be altered by using the force convection method to increase the heat transfer. Ahmad and Qureshi (1992) examined the mixed convection heat transfer from a horizontal cylinder subjected to the uniform heat flux. The simulation has been done for fluid Prandtl number 0.7 and the Reynolds number ranged from 1 to 60 and the modified Grashof numbers between 0 and 1.6×10^4. They found out that a uniform heat flux cylinder dissipates more heat than the same one under the uniform surface temperature boundary condition. Moreover, the heat transfer and drag coefficients in the mixed convection regime remarkably increased in comparison with the values that could exist in pure forced convection. In another research study, Elsayed *et al*. (2003) reported an experimental investigation on free convection of air around the outer surface of a constant heat flux elliptic tube. The local and average Nusselt numbers have been calculated for various Rayleigh number and tube inclination angles. The results revealed that a higher value of average Nusselt number is achieved when the major axis of the tube is vertical. They proposed an empirical correlation to evaluate the average Nusselt number in terms of the Rayleigh number based on the input heat flux. A voluminous literature exists in the flow and heat transfer characteristics past over semicircular, triangular and square cylinder (Nada and Mowad 2003, Kumar De and Dalal 2006, Chandra and Chhabra 2011, Sasmal and Chhabra 2011).

Employing nanofluid for the purpose of increasing the heat transfer in thermal systems is an alternative

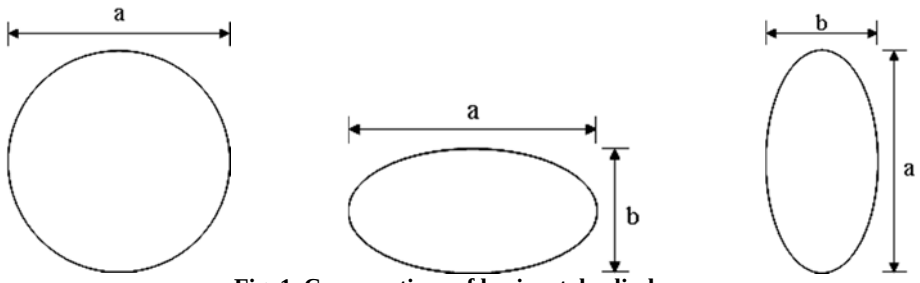

Fig. 1. Cross sections of horizontal cylinder.

technique which draws serious attention. The thermal performance of different types of nanofluid has been the subject of many recent studies on forced, natural, and mixed convection problems (Chol 1995, Sidik, Khakbaz *et al*. 2013). Sarkar *et al*. (2012) studied the buoyancy driven mixed convective flow and heat transfer characteristics of the water-based copper nanofluid past a circular cylinder. The Reynolds number of the flow considered as $80 \leq \mathrm{Re} \leq 180$ and the volume fraction of the nano particles assumed as $0 \leq \emptyset \leq 25\%$. Effect of buoyancy force has been analyzed by considering two particular Richardson numbers of 1 and -1. The results show that the average Nusselt number increases with particle volume fraction and Reynolds number enhancement. They reported a detailed analysis of vortex formation and drag force variation in different particle concentration. A numerical investigation of the heat transfer phenomena over an isothermal cylinder, for low Reynolds number flow of water based copper nanofluid has been done by Vegad *et al*. (2014). They found out that the heat transfer coefficient increases by solid fraction enhancement, which could be the results of thermal conductivity improvement. In addition, by increasing the nano particle volume fraction, the temperature gradient and heat flux decline at the cylinder surface along normal direction and toward the rear stagnation point respectively.

The heat transfer procedure is normally accompanied by thermodynamic irreversibility or entropy generation. All the above mentioned studies concerns about the energy analyses based on the first law, however the first law analysis does not explain the irreversibility or degradation of energy in the system. The energy quality analysis is a relatively modern method to provide an effective way to optimize the performance of a thermal system based on the principle of entropy generation minimization. Yang *et al*. (2007) analyzed the entropy generation of the laminar film condensation on an ellipsoid under the effect of the non-isothermal wall temperature for different ellipticity. The results illustrated that, the entropy generation due to heat transfer in comparison to the film flow friction is superior in most cases. Moreover, the entropy generation enhances by the ellipticity of ellipsoid. The entropy generation and exergy destruction of a magnetic nanofluid in curved rectangular microchannel have been investigated by Mohammadpour *et al*. (2015). They reported that the generated entropy due to the flow friction is negligible compared to the heat transfer entropy generation. In addition, the results indicated that the entropy generation is decreased by increasing the curvature angle of microchannel and nonuniform transverse magnetic field intensity.

In this paper, natural and mixed convective flow and heat transfer characteristics of the water-based Al_2O_3 nanofluid past a horizontal cylinder with three circular, horizontal and vertical elliptical cross sections have been investigated. The study has been performed by the assumption of a laminar steady flow over a cylinder with a uniform surface temperature of T_s ($T_s > T_\infty$), the Rayleigh number of Ra=42240 and Reynolds number Re=93. The objective of the current study is to examine the influence of the upstream flow direction and the nanoparticles volume fraction on the heat transfer characteristic in natural and mixed convective flow. In addition, in the present study the entropy generation analysis has been done by considering the effect of geometry variation and addition of nano-sized particles into the base fluid. The entropy generation and energy dissipation due to the heat transfer and flow friction irreversibility have been investigated as well.

2. PROBLEM DEFINITION

The geometrical configuration for the current study consists of a horizontal cylinder with three different cross sections of circular, horizontal and vertical ellipses. The minor and major axis ratios of the elliptical cross-section of the cylinder considered b/a=0.5 as it is shown in Fig. 1.

A schematic diagram of the considered free and mixed convection mechanisms in this research is shown in Fig. 2. The heat transfer mechanisms which are shown in this figure can be defined as follows:

Type1: The mixed convection of flow when the free convection acts in the opposite direction to the forced convection

Type2: The mixed convection of flow when the free convection acts perpendicular to the force convection

Type3: The mixed convection of flow when the natural and force convective flow occur in the same direction.

Heat transfer occurs between the cylinder with a uniform surface temperature of T_s and the surrounding fluid of temperature T_∞. The length of

Table 1 Dimensionless parameters used in the non-dimensional equations

Dimensionless variable	Mixed convection	Free convection
Length	X= x/a , Y= y/a	X= x/a , Y= y/a
Velocity	U= u/$\mathbf{u}_\infty$, V= v/$\mathbf{u}_\infty$	U= ua/α , V= va/α
Pressure	$P=\frac{p}{\rho u_\infty^2}$	$P=\frac{pa^2}{\rho\alpha^2}$
Temperature	$\theta=\frac{T-T_\infty}{T_s-T_\infty}$	$\theta=\frac{T-T_\infty}{T_s-T_\infty}$

the cylinder assumed long enough compared to its diameter to make sure that the normal gradient of temperature and velocity field are negligible and 2D computational method obtain an acceptable accuracy. In addition, the problem is solved based on the assumption of laminar, steady incompressible flow. The convection heat transfer simulation has been performed by adopting a homogeneous single phase modeling approach for nanofluid. The fluid phase and nanoparticles are assumed to be in thermal equilibrium state and flow at the same velocity. The thermo-physical properties of the nano-fluid are considered to be constant except the density, which is calculated based on the Boussinesq approximation. The pressure work and viscous dissipation are ignored as well.

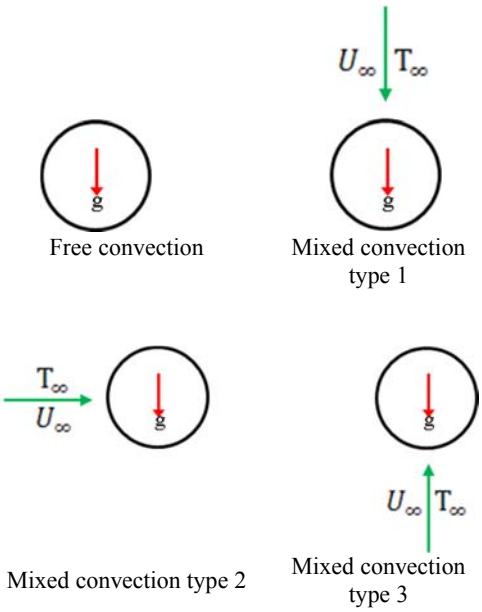

Fig. 2. Different kinds of convection heat transfer mechanisms were considered in this study.

Nowadays a wide variety of relations for calculating the thermo physical properties of nanofluid and two phase models has been reported. It has been established that their accuracy for solving the free convection problem, especially in cases which are related to nanofluid, is almost the same. Based on the results of Abouali and Ahmadi (2012), applying a homogeneous single phase model for classic problem in the current study is valid. Moreover, due to the simplicity of Al_2O_3 nanofluid preparation, its employment in a wide range of applications and referring to the discussion in (Abouali and Ahmadi 2012), this kind of nanoparticle has been selected.

3. GOVERNING EQUATIONS AND NUMERICAL FORMULATION

3.1 Governing Equation

Dimensionless governing equations of steady, laminar and two-dimensional incompressible flows with convection heat transfer using Boussinesq approximation are as follows (Bejan 2013):

$$\frac{\partial U}{\partial X}+\frac{\partial V}{\partial Y}=0 \tag{1}$$

$$U\frac{\partial U}{\partial X}+V\frac{\partial U}{\partial Y}=-\frac{\partial P}{\partial X}+\lambda_1\left(\frac{\partial^2 U}{\partial X^2}+\frac{\partial^2 U}{\partial Y^2}\right) \tag{2}$$

$$U\frac{\partial V}{\partial X}+V\frac{\partial V}{\partial Y}=-\frac{\partial P}{\partial Y}+\lambda_1\left(\frac{\partial^2 V}{\partial X^2}+\frac{\partial^2 V}{\partial Y^2}\right)+\lambda_2\theta \tag{3}$$

$$U\frac{\partial \theta}{\partial x}+V\frac{\partial \theta}{\partial Y}=\lambda_3\left(\frac{\partial^2 \theta}{\partial X^2}+\frac{\partial^2 \theta}{\partial Y^2}\right) \tag{4}$$

Entropy generation of heat and friction are calculated by the following formula (Bejan 1982, Bejan 1996, Bejan 2016):

$$\dot{S}_{gen,\Delta T}=\frac{K}{T0^2}\nabla^2 T \tag{5}$$

$$\dot{S}_{gen,\Delta P}=\frac{\mu}{T0}\left[\frac{\partial u_i}{\partial x_j}+\frac{\partial u_j}{\partial x_i}\right]\frac{\partial u_i}{\partial x_j} \tag{6}$$

Where K is the thermal conductivity and μ is the viscosity of the fluid. T_0 is the average temperature of control volume.

Dimensionless variables in natural and mixed convective flow have been defined as it is mentioned in Table 1.

λ coefficient in non-dimensional equations of natural and mixed convection heat transfer are defined as Table 2.

Table 2 Lambda coefficient in different convection heat transfer

Convective heat transfer	$\boldsymbol{\lambda_1}$	$\boldsymbol{\lambda_2}$	$\boldsymbol{\lambda_3}$
Free convection	Pr	Ra×Pr	1
Mixed convection	$\mathbf{Re^{-1}}$	$\frac{\mathbf{Ra}}{\mathbf{Re^2\times Pr}}$	$\frac{\mathbf{1}}{\mathbf{Re\times Pr}}$

Table 3 Thermo-Physical properties of base fluid and the nanoparticles (Boukerma and Kadja 2017)

Thermo-physical properties	water	Al_2O_3
Density ($\mathbf{kg/m^3}$)	993.04	3600
Specific heat capacity (j/kg k)	4178	765
Thermal conductivity (w/m.k)	0.628	36
Dynamic viscosity ($\mathbf{Ns/m^2}$)	$\mathbf{695 \times 10^{-6}}$	-
Thermal expansion coefficient (1/k)	$\mathbf{361.9 \times 10^{-6}}$	$\mathbf{5.8 \times 10^{-6}}$

The dimensionless variables which are used in λ definition are as follows:

Ra= $\frac{g\beta(T_s-T_\infty)a^3}{\nu\alpha}$, $Re=\frac{\rho u_\infty a}{\mu}$, Pr= $\frac{\nu}{\alpha}$

The boundary conditions in natural and mixed convection are considered as:

Free convection:

$U=0$ ،$V=0$ ، $\theta=1$ on cylinder surface

$U=0$ ،$V=0$ ، $\theta=0$ far away from the cylinder surface

Mixed convection:

$U=0$ ،$V=0$ ، $\theta=1$ on cylinder surface

$U=1$ ،$V=0$ ، θ=0 far away from the cylinder surface

3.2 Thermo-Physical Properties of NanoFluid

By including the nanofluid into the based fluid, due to the existence of the inter-particle forces, the nanofluid shows different behavior from the pure fluid. It provides higher efficiency in energy transport alongside the better stabilization than the ordinary solid–liquid mixture. In order to solve the second distribution function for energy evolution, thermal properties of fluid such as thermal conductivity, heat capacitance and thermal expansion are required to be changed. The effective density of a fluid containing suspended particles at a reference temperature is given by:

$$\rho_{nf}=(1-\varphi)\rho_f+\varphi\rho_p \quad (7)$$

Where ϕ is the volume fraction of nanoparticles.

$$\varphi=\frac{volume\ of\ nanoparticles}{total\ volume\ of\ solution} \quad (8)$$

The effective thermal conductivity can be computed according to the (Li, Xuan *et al.* 2003):

$$(\rho c_p)_{nf}=(1-\varphi)(\rho c_p)_f+\varphi(\rho c_p)_p \quad (9)$$

The effective viscosity for nanofluid which is consisting of pure water with viscosity μ_f and a dilute suspension of small solid spherical particles at a very low volume fraction is given by Einstein in 1906 as (1906):

$$\mu_{nf}=(1+2.5\ \varphi)\mu_f \quad (10)$$

Batchelor (1977) modified Einstein's viscosity equation by introducing Brownian motion effect. The model was developed by considering isotropic suspension of rigid and spherical nanoparticles:

$$\mu_{nf}=(1+2.5\ \varphi+6.2\varphi^2)\mu_f \quad (11)$$

A noticeable number of studies have been reported about the effects of particle size, particle shape, volume fraction and temperature on the viscosity of nanofluids. A brief review of nanofluid viscosity computation methods has been reported by Mishra *et al.* (2014). Prasher *et al.* (2006) performed an experimental study on the viscosity of alumina-based nanofluids for various shear rates, temperature, nanoparticle diameter, and nanoparticle volume fraction. Based on these studies the viscosity in low volume fraction can be calculated using Einstein suggested formula while in a high volume fraction of nanoparticles, in which the particle aggregation happens, the formula is no longer valid. In the current study, we considered a dilute suspension of nanoparticles and Einstein formula for nanofluid viscosity calculation.

The thermal expansion of the nanofluid can be determined as:

$$\beta_{nf}=(1-\varphi)\beta_f+\varphi\beta_p \quad (12)$$

The effective stagnant thermal conductivity of the solid–liquid mixture is computed using the Maxwell–Garnett's model (Tiwari and Das 2007) for the two phase flow of spherical-particle suspension:

$$k_{nf}=\left[\frac{k_{p+2k_f+2\varphi(k_p-k_f)}}{k_p+2k_f-\varphi(k_p-k_f)}\right]k_f \quad (13)$$

which in all equations the nf, f and p indices belong to the nanofluid, base fluid and nanoparticles properties respectively. Thermo-physical properties of nanoparticles and base fluid in 310 K are mentioned in Table 3 (Boukerma and Kadja 2017).

The average Nusselt number on the surface of cylinder as an index of the heat transfer rate can be calculated as:

$$Nu=\frac{ha}{k} \quad (14)$$

It should be noted that the K in the above relation is thermal conductivity of the nanofluid. The major axis of the ellipse for elliptical cross sections is called a and h is the average convective heat transfer coefficient given as:

$$h=\frac{\bar{q}}{(T_s-T_\infty)} \quad (13)$$

$\bar{q}$ is the average heat flux on the cylinder surface.

Numerical Method

The aforementioned set of coupled nonlinear

Table 4 Numerical validation for cylinder surface average Nusselt number

Cylinder cross section	Reported Nusselt by (Corcione and Habib 2009)	Reported Nusselt by (Cianfrini, Corcione *et al*. 2006)	Current study
Circular	-	8.035	8.014
Horizontal ellipse	7.82	-	7.98
Vertical ellipse	9	-	9.12

differential equations has been discretized and solved by using the control volume technique. For the convective and diffusive terms a first order upwind method has been used while the SIMPLE procedure has been introduced for the velocity–pressure coupling. The convergence criteria assumed to be 10^{-5} in all calculations.

3.3 Mesh Independency and Numerical Method Validation

Figure 3 shows the computational domain and structured non-uniform grids which have been used to discretize the computational domain. The meshes are finer in the vicinity of the wall where more accurate solutions are required. The maximum and minimum diameters of the cylinder have been adjusted to D and 2D, also the dimension of computational domain has been considered as 50D*50D.

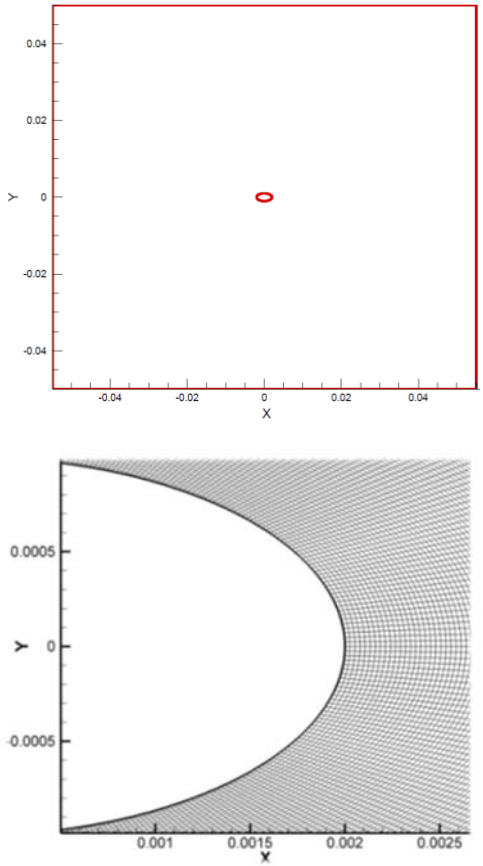

Fig. 3. Typical grid and computational domain.

The grid independency simulations have been performed based on the average Nusselt number on the cylinder surface in Ra=101440 and Pr=0.7. The results are shown in Table 5, 6 and 7 for horizontal cylinders of circular, horizontal and vertical cross section respectively. According to the results, the grid-independent situation was achieved for all simulations of the current study in 400*300, 400*450 and 400*250 meshes for slender ellipse, blunt ellipse and circular cross sections respectively.

Table 5 Average Nusselt number on the circular cylinder for the grid examination

Mesh number	Average Nusselt Number
400×125	8.3
400×150	8.2
400×175	8.2
400×200	8.1
400×250	8.2
400×300	8.0
400×325	8.0

Table 6 Average Nusselt number on the cylinder surface of blunt ellipse cross section for the grid examination

Mesh number	Average Nusselt Number
400×125	8.4
400×150	8.3
400×175	8.2
400×200	8.2
400×250	8.1
400×300	8.1
400×375	8.0
400×450	8.0
400×500	8.0

Table 7 Average Nusselt number on the cylinder surface of slender ellipse cross section for the grid examination

Mesh number	Average Nusselt Number
400×125	9.3
400×150	9.2
400×175	9.2
400×200	9.2
400×250	9.1
400×300	9.1

Table 8 Average Nusselt number of free convection heat transfer for different cross sections

Cylinder cross section	The nanoparticles volume fraction	The average Nusselt number
Circular	0	7.6
	0.01	7.5
	0.02	7.5
	0.03	7.4
Horizontal ellipse	0	7.8
	0.01	7.7
	0.02	7.6
	0.03	7.5
Vertical ellipse	0	8.9
	0.01	8.8
	0.02	8.7
	0.03	8.6

To validate the numerical method, the free convection over a cylinder with a uniform surface temperature for three different cross sections of circular, horizontal and vertical ellipse has been simulated. The average Nusselt number on the surface of the cylinder for Ra= 101440 and Pr=0.7 has been calculated. This value was compared with the results of (Corcione and Habib 2009) for vertical and horizontal ellipse and validated with the result of (Cianfrini, Corcione *et al*. 2006) for circular cross section. The obtained results are illustrated in Table 4. Agreements are probably as good as one may hope for.

The thermal and hydro dynamical behavior of mixed convective flow are affected by the wide range of nondimensionalized parameters like Re, Ra, Nu, Pe, Pr, and etc., which investigating the influence of each factor variation on the characteristic of the flow may lead to a vast collection of studies. The main goal of this work is to investigate the heat transfer and thermodynamic irreversibility rates of different natural and mixed convection mechanisms of nanofluid flow past a cylinder with different cross section in specific Re and Ra numbers.

4. RESULTS AND DISCUSSIONS

In the present study, the entropy generation and heat transfer of water based Al_2O_3 nanofluid through the natural and mixed convective flow past a horizontal cylinder with different cross sections have been studied numerically. The cylinder cross sections are shown in Fig. 1. It should be mentioned that, the minor and major axis ratios of the elliptical cross-section of the cylinder considered as b/a=0.5 and the volume fraction of the nanoparticles supposed to be in the range of $0.01 \leq \phi \leq 0.03$.

The mixed convection heat transfer for three different configurations which are shown in Fig. 2 at the fixed Ra=42240, Re=93, Gr=9324 and Pr=4.5 has been studied.

The Reynolds and Rayleigh numbers are calculated based on the thermo-physical properties of pure fluid. These quantities are considered in order to the buoyancy and inertia forces be equal, in other words, the Richardson number be equal to one (Gr/Re2=1). The Nu number is calculated based on the thermal conductivity of the nanofluid. Also it should be mentioned that Ra, Nu and Re numbers are calculated based on the major axis of the ellipse for elliptical cross sections. The results show that the average Nusselt number variation due to the nanoparticle addition in base fluid in all cases of natural and mixed convection heat transfer follows the same trend. By this mean, by enhancing the volume fraction of nanoparticles in the base fluid the value of the average Nusselt number in all cases decreases while the heat transfer rate increases as shown in Table 8, 9, 10 and 11 for free convection, mixed convection type 1, type 2 and type 3 respectively. Thermal conductivity of nanofluid is higher than the thermal conductivity of pure fluid which leads to adverse relation between Nu and h. Evidently, both diffusion and convective flow mechanisms take effect on heat transfer and Nu number values which their influences can be pointed out by Peclet number. Pure convection is fundamentally based on the density difference due to temperature gradient and body force. By adding nanoparticles, the weighted flow cannot easily stimulate and replace under the influence of specific temperature gradient and boundary condition. Besides, increasing the volume fraction of nanoparticles causes an enhancement in both viscosity and thermal conductivity of the fluid. Increasing the volume fraction of nanoparticles augments the thermal conductivity of the fluid which is resulted in heat transfer improvement. By increasing viscosity, the thickness of thermal boundary layer is increased and hence, the temperature gradient near the cylinder is decreased which causes the Nu number reduction. The combination of these contradicting effects defines the characteristics of heat transfer which could be resulted in increasing or declining the Nu number as it has been reported in several studies.

In the current study, based on the results, the average Nusselt number in all convective heat transfer

Table 9 Average Nusselt number of mixed convection heat transfer type 1 for different cross sections

Cylinder cross section	The nanoparticles volume fraction	The average Nusselt number
Circular	0	8.1
	0.01	8.0
	0.02	7.9
	0.03	7.8
Horizontal ellipse	0	9.4
	0.01	9.3
	0.02	9.2
	0.03	9.0
Vertical ellipse	0	9.5
	0.01	9.4
	0.02	9.3
	0.03	9.1

Table 10 Average Nusselt number of mixed convection heat transfer type 2 for different cross sections

Cylinder cross section	The nanoparticles volume fraction	The average Nusselt number
Circular	0	12.592
	0.01	12.43
	0.02	12.281
	0.03	12.127
Horizontal ellipse	0	13.15
	0.01	12.99
	0.02	12.83
	0.03	12.683
Vertical ellipse	0	15.94
	0.01	15.72
	0.02	15.51
	0.03	15.3

Table 11 Average Nusselt number of mixed convection heat transfer type 3 for different cross sections

Cylinder cross section	The nanoparticles volume fraction	The average Nusselt number
Circular	0	11.093
	0.01	10.966
	0.02	10.843
	0.03	10.719
Horizontal ellipse	0	12.329
	0.01	12.19
	0.02	12.059
	0.03	11.936
Vertical ellipse	0	13.418
	0.01	13.26
	0.02	13.113
	0.03	12.96

mechanisms and all volume fractions of nanoparticles for slender ellipse is larger than the blunt ellipse and circular cross section which could be related to the large area of stagnant points in the

front and rear of the cylinder (Corcione and Habib 2009).

The comparative results illustrated that in all simulated cases of different volume fraction and various cross sections, the Nusselt number in the mixed convection heat transfer of type 2 is larger than the others.

As it has been mentioned before, adding the nanoparticles in both free and mixed convection, due to the fluid thermal conductivity enhancement, leads to the heat transfer rate increase with regard to the pure fluid in specific boundary conditions. The average heat transfer rate variations due to the particle volume fraction for all case studies are shown in Fig. 4, 5, 6 and 7. According to the Fig. 4 and 5, it is observed that the results of free convection average heat transfer rate for cylinder with horizontal ellipse cross section are almost the same as circular one and in mixed convection type 1, the corresponding values are similar to the cylinder with vertical elliptical cross section. It is noticeable that, as it is shown in Fig. 7, the minimum amount of heat transfer rate in mixed convection of type 3 is more than the maximum value of that in natural and mixed convection type1.

Based on the comparison of Fig. 4, 5 and 6, 7 it is obvious that the best option for improving the heat transfer is the mixed convection heat transfer of type 2. Pursuant to the flow direction, the force flow is agitated the main stream in heat transfer type 2. This agitation disturbs the insulating blanket around the cylinder. Continues disturbance of the boundary layer increases the amount of turbulence within the fluid and heat is transferred more effectively.

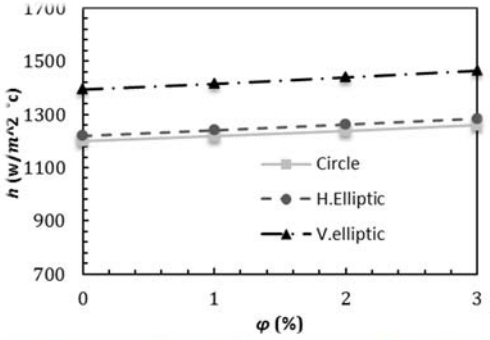

Fig. 4. Convection heat transfer coefficient for pure free convection.

As it is noticed before, in the current study in addition to the study of the external mixed convective heat transfer for pure and nanofluid flow over a cylinder with different cross sections, the second law of thermodynamic or the entropy generation analysis which is proportional to the irreversibility has been investigated. Due to the fact that, the maximum friction entropy generation is of order of 10^{-4} and in compare with the thermal entropy production is negligible, hence in the current study the total entropy is considered equivalent to the heat transfer generated entropy (Yang, Hung *et al*. 2007).

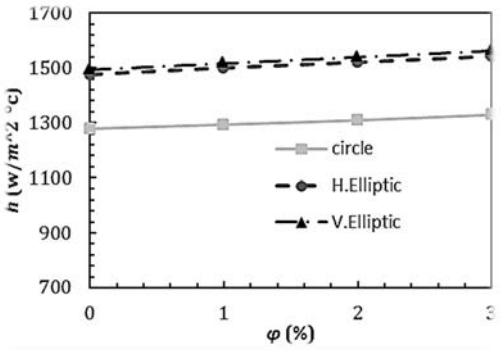

Fig. 5. convection heat transfer coefficient for combined convection type 1.

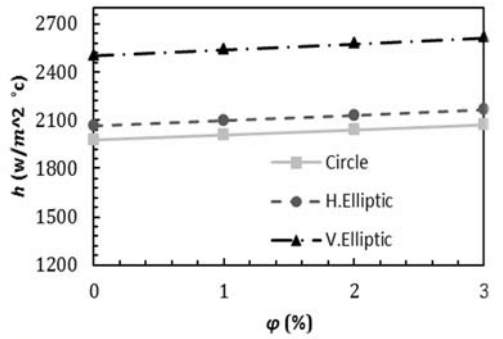

Fig. 6. Convection heat transfer coefficient for combined convection type 2.

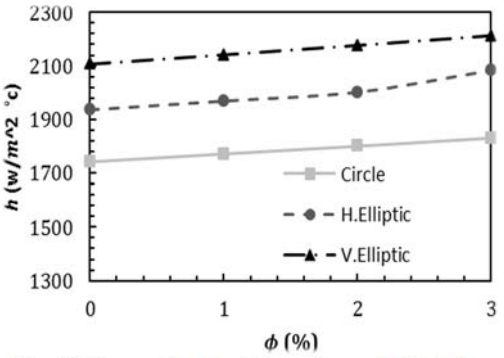

Fig. 7. Convection heat transfer coefficient for combined convection type 3.

The entropy generation for pure fluid and nanofluid with $\phi = 0.03$ is shown in Fig. 8. In this fig. horizontal axis represents the cross sections geometries and numbers 1, 2 and 3 respectively indicate the circular, blunt and slender ellipse cross section. According to this figure, it is illustrated that by adding the nanoparticles to the base fluid the entropy generation increased slightly. A careful inspection shows that this raise is more perceptible in slender ellipse cross section. Moreover, in all mechanism of heat transfer the entropy generation in cylinder with vertical ellipse cross section is more than the horizontal ellipse and circular ones.

Based on the equations 5 and 6 the generation of entropy is owing to the velocity gradient (strain rate) in frictional part and the temperature gradient in

thermal part. In this study, the laminar mixed convection and constant wall temperature boundary condition on the cylinder induce a bit difference between the temperature and velocity gradient in case of pure and nanofluid flow field.

According to the figures, the entropy production in all three cross sections for mixed convection heat transfer type 2 has the maximum value and for the free convection is the lowest. Analyzing the Figs. 4 to 8 simultaneously, illustrates that however in all heat transfer mechanisms the rate of heat transfer in slender ellipse is more than blunt ellipse and circular cross section, the entropy generation in this cross section is much more than the others as well. According to the result, using the slender ellipse in the best case could increase the heat transfer rate by 20%, while in almost all heat transfer mechanisms; it produces irreversibility more than 40-50% in comparison with circular and horizontal cross sections.

As an example, considering the Figs. 8 and 5, indicates that the entropy generation in mixed convection heat transfer type 1 for the cylinder with slender ellipse cross section is almost twice the cylinder with blunt ellipse cross section while the rate of heat transfer in both geometries is almost the same.

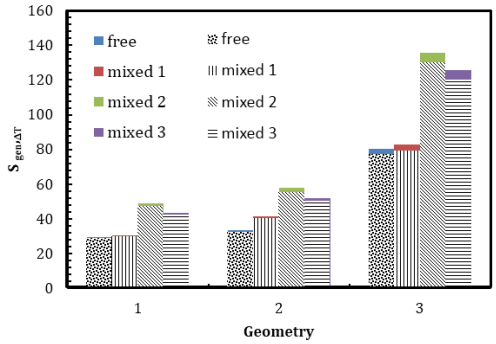

Fig. 8. Heat transfer entropy generation for pure fluid (shaded) and nanofluid (colorful).

Increasing the volume fraction of nanofluid leads to heat transfer enhancement between hot and cold sections, which it is one of the most important causes of irreversibility. In our case, the uniform temperature boundary condition on cylinder wall has the most significant influence on the low rate of entropy generation increase. In all processes, the case of minimum entropy generation is preferable (because of avoiding the irreversibility), but the situation does not correspond to the best heat transfer condition possibly. Thus, according to the priorities and constraints which should be taken into account and the results, the optimal case could be selected by combining the first law and second law of thermodynamics and determining the actual performance of heat transfer.

Regarding to the fact that the entropy contour in $\phi = 0$ is under the influence of the isotherms, in Fig. 9 the temperature contour for different cross sections and various heat transfer mechanisms are shown for $\phi = 0.03$. The solid lines represent the pure fluid and the dashed lines represent the nanofluid by a nanoparticles volume fraction of $\phi = 0.03$.

According to the figures it is seen that the contours of isotherm on the vicinity of the surface of the cylinders in all cases are matches for both pure and nanofluid, while by distancing from the surface some differences appear. It should be mentioned that, when the temperature gradient increases, the entropy generation due to Eq. 6 and thermo physical properties (which are enhanced in the presence of nanoparticles) is faced to alteration.

According to the figures in all mechanisms of mixed convection the thickness of the temperature distribution area is elongated in the downstream region corresponding to the forced flow direction. The forced flow induces the change in direction or velocity of the flow. This phenomenon is more obvious in mixed convection type 1. The contra flow causes an adverse pressure gradient and increases the fluid flow, which inhibits the flow field to be separated from the surface of the cylinder. In contrast to the parallel flow and natural convective flow the point of separation occurs quickly, and the size of the vortex is large for contra flow under the same boundary conditions.

5. CONCLUSION

In this study, natural and mixed convective flow and heat transfer characteristics of the water-based Al_2O_3 nanofluid past a horizontal cylinder with three circular, horizontal and vertical elliptical cross sections have been investigated numerically. The study has been performed by the assumption of a laminar steady flow over a cylinder with a uniform surface temperature of T_s ($T_s > T_\infty$), the Rayleigh number of Ra=42240 and Reynolds number Re=93. The effect of different parameters, such as cylinder cross section and nanoparticles volume fraction and the upstream flow direction in mixed convection, on the rate of heat transfer and entropy generation have been studied. The result can be concluded as follows:

In all simulated cases of different cross sections, the Nusselt number and entropy generation in the mixed convection heat transfer of type 2 is larger than the others.

In all mechanisms of heat transfer, the entropy generation and Nusselt number in a cylinder with vertical ellipse cross section are more than the horizontal ellipse and circular ones.

In all mechanisms of heat transfer, by adding the nanoparticles to the base fluid and increasing the particles volume fraction the rate of the heat transfer enhances corresponding to the convective heat transfer improvement. Moreover, increasing the nanoparticle volume fraction results in the Nusselt number reduction and entropy generation augmentation.

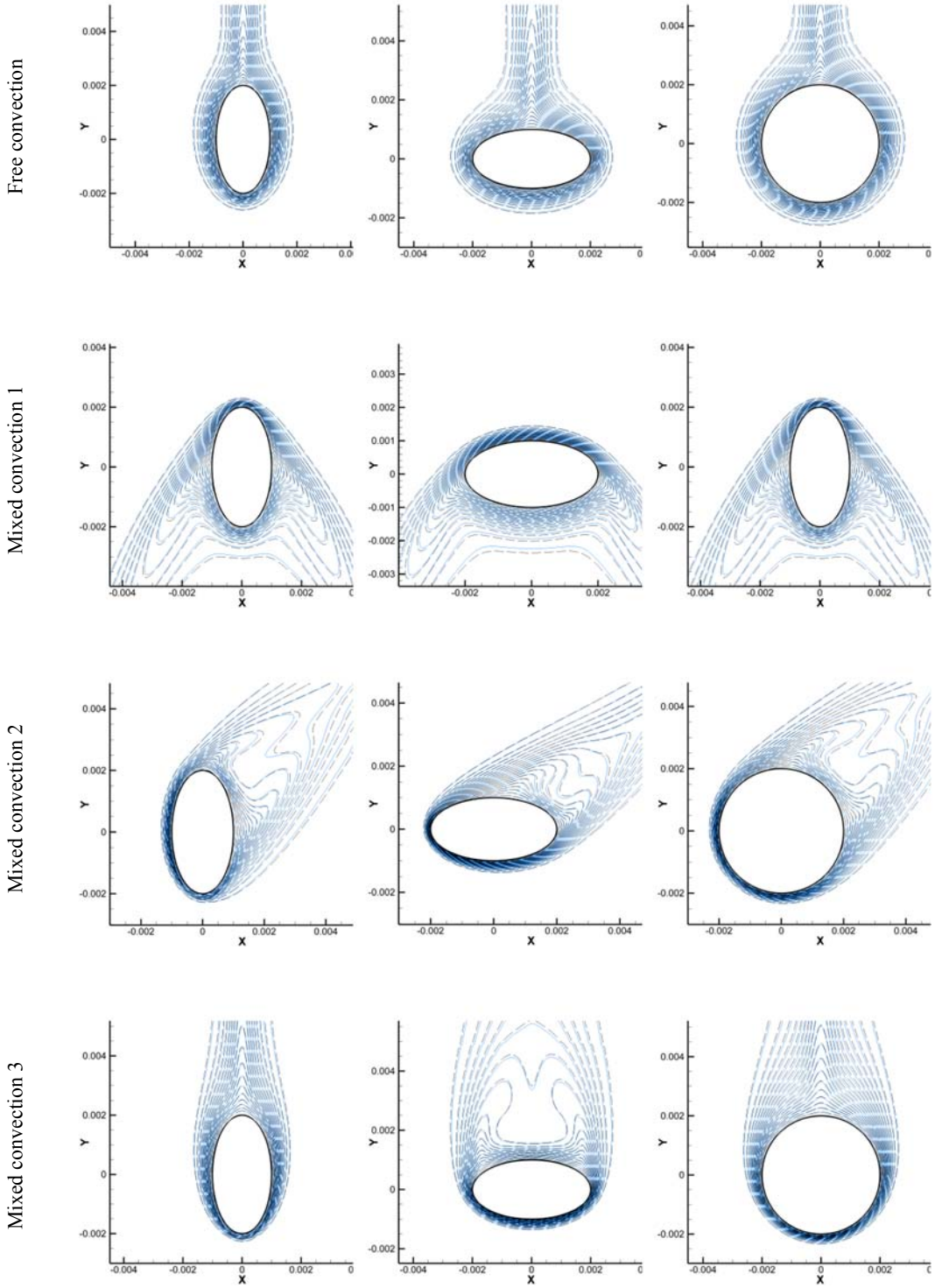

Fig. 9. Constant temperature contour of pure fluid in comparison to the nanofluid (3% *V*. *F*) for 4 types of convection heat transfer.

Generating the forced convection even in the opposite direction of the natural and buoyant flow increases the heat transfer rate and Nusselt number.

The contours of isotherm on the vicinity of the surface of the cylinders in all cases are almost matches for both pure and nanofluid. By neglecting the entropy generation caused by friction, thermal entropy generation value directly relates to the temperature gradient. Due to a little temperature difference, total entropy generations of pure and nanofluid cases are similar.

The generated entropy value is proportional to the irreversibility, consequently the thermodynamics cycles have should avoid it. The result of current study indicated that the entropy generation due to the temperature gradient and alteration in thermo physical properties changes the heat transfer coefficient. Hence, the convective heat transfer rate enhancement takes place despite the fact that the irreversibility occurs in flow field as well. All methods involved in increasing the heat transfer coefficient e.g. adding nanoparticles, cross section variation, using mixing mechanism, installing fins, applying external forces like magnetic-electric field and etc. augment the heat transfer rate with the aid of entropy generation.

The simulations in the current study have been performed for the convective flow past a cylinder while flow over the tube bundle with different configuration is more practical in industries due to the interaction of the flow past the cylinders. Therefore, the convective flow for different configuration of a tube bundle will be investigated in our future study by considering the entropy generation value and exergy analysis.

REFERENCES

Abouali, O. and G. Ahmadi (2012). Computer simulations of natural convection of single phase nanofluids in simple enclosures: a critical review. *Applied Thermal Engineering 36*, 1-13.

Ahmad, R. and Z. Qureshi (1992). Laminar mixed convection from a uniform heat flux horizontal cylinder in a crossflow. *Journal of thermophysics and heat transfer 6*(2), 277-287.

Badr, H. M. (1994). Mixed convection from a straight isothermal tube of elliptic cross-section. *International Journal of Heat and Mass Transfer 37*(15), 2343-2365.

Batchelor, G. (1977). The effect of Brownian motion on the bulk stress in a suspension of spherical particles. *Journal of fluid mechanics 83*(01), 97-117.

Bejan, A. (1982). *Entropy generation through heat and fluid flow*. Wiley.

Bejan, A. (1996). Entropy generation minimization: The new thermodynamics of finite-size devices and finite-time processes. *Journal of Applied Physics 79*(3), 1191-1218.

Bejan, A. (2013). *Convection Heat Transfer*, John wiley & sons.

Bejan, A. (2016). *Advanced Engineering Thermodynamics*, John Wiley & Sons.

Boukerma, K. and M. Kadja (2017). Convective Heat Transfer of Al2O3 and CuO Nanofluids Using Various Mixtures of Water-Ethylene Glycol as Base Fluids. *Engineering, Technology & Applied Science Research 7*(2), pp. 1496-1503.

Chandra, A. and R. P. Chhabra (2011). Flow over and forced convection heat transfer in Newtonian fluids from a semi-circular cylinder. International *Journal of Heat and Mass Transfer 54*(1–3), 225-241.

Chol, S. (1995). Enhancing thermal conductivity of fluids with nanoparticles. *ASME-Publications*-Fed 231, 99-106.

Cianfrini, C., M. Corcione and E. Habib (2006). Free convection heat transfer from a horizontal cylinder affected by a downstream parallel cylinder of different diameter. *International Journal of Thermal Sciences 45*(9), 923-931.

Corcione, M. and E. Habib (2009). Multi-Prandtl correlating equations for free convection heat transfer from a horizontal tube of elliptic cross-section. *International Journal of Heat and Mass Transfer 52*(5), 1353-1364.

Dawood, H. K., H. A. Mohammed, N. A. Che Sidik, K. M. Munisamy and M. A. Wahid (2015). Forced, natural and mixed-convection heat transfer and fluid flow in annulus: A review. *International Communications in Heat and Mass Transfer 62*, 45-57.

Einstein, A. (1906). Eine neue bestimmung der moleküldimensionen. *Annalen der Physik 324*(2), 289-306.

Elsayed, A. O., E. Z. Ibrahim and S. A. Elsayed (2003). Free convection from a constant heat flux elliptic tube. *Energy Conversion and Management 44*(15), 2445-2453.

Garoosi, F., L. Jahanshaloo and S. Garoosi (2015). Numerical simulation of mixed convection of the nanofluid in heat exchangers using a Buongiorno model. *Powder Technology 269*, 296-311.

Huang, S. Y. and F. Mayinger (1984). *Heat and Mass Transfer 18*(3), 175-183.

Kang, G. U. and B. J. Chung (2012). Influence of the height-to-diameter ratio on turbulent mixed convection in vertical cylinders. *Heat and Mass Transfer 48*(7), 1183-1191.

Krishne Gowda, Y. T., P. A. Aswatha Narayana and K. N. Seetharamu (1996). Numerical investigation of mixed convection heat transfer past an in-line bundle of cylinders. *Heat and Mass Transfer 31*(5), 347-352.

Kumar De, A. and A. Dalal (2006). Numerical Study of Laminar Forced Convection Fluid Flow and Heat Transfer From a Triangular Cylinder Placed in a Channel. *Journal of Heat Transfer 129*(5), 646-656.

Li, Q., Y. Xuan and J. Wang (2003). Investigation on convective heat transfer and flow features of nanofluids. *Journal of Heat transfer 125*(2003), 151-155.

Lin, F. and B. Chao (1976). Addendum:Laminar Free Convection Over Two-Dimensional and Axisymmetric Bodies of Arbitrary Contour, Journal of Heat Transfer, 1974, 96, pp. 435–

442). *Journal of Heat Transfer 98*(2), 344-344.

Merkin, J. H. (1977). Free Convection Boundary Layers on Cylinders of Elliptic Cross Section." *Journal of Heat Transfer 99*(3), 453-457.

Mishra, P. C., S. Mukherjee, S. K. Nayak and A. Panda (2014). A brief review on viscosity of nanofluids. *International nano letters 4*(4), 109-120.

Mohammadpourfard, M., S. A. Zonouzi and F. Mohseni (2015). Numerical Study of the Hydrothermal Behavior and Exergy Destruction of Magnetic Nanofluid in Curved Rectangular Microchannels. *Heat Transfer Research 46*(9).

Nada, S. and M. Mowad (2003). Free convection from a vertical and inclined semicircular cylinder at different orientations. *Alexandria Engineering Journal 42*(3), 273-282.

Prasher, R., D. Song, J. Wang and P. Phelan (2006). Measurements of nanofluid viscosity and its implications for thermal applications. *Applied physics letters 89*(13), 133108.

Sarkar, S., S. Ganguly and G. Biswas (2012). Mixed convective heat transfer of nanofluids past a circular cylinder in cross flow in unsteady regime. *International Journal of Heat and Mass Transfer 55*(17), 4783-4799.

Sasmal, C. and R. P. Chhabra (2011). Laminar natural convection from a heated square cylinder immersed in power-law liquids. *Journal of Non-Newtonian Fluid Mechanics 166*(14–15), 811-830.

Shin, S. C. and K. S. Chang (1989). Transient natural convection heat transfer from a horizontal circular cylinder. *International communications in heat and mass transfer 16*(6), 803-810.

Sidik, N. A. C., M. Khakbaz, L. Jahanshaloo, S. Samion and A. N. Darus (2013). Simulation of forced convection in a channel with nanofluid by the lattice Boltzmann method. *Nanoscale research letters 8*(1), 1-8.

Terukazu, O., N. Hideya and T. Yukiyasu (1984). Heat transfer and flow around an elliptic cylinder. *International Journal of Heat and Mass Transfer 27*(10), 1771-1779.

Tiwari, R. K. and M. K. Das (2007). Heat transfer augmentation in a two-sided lid-driven differentially heated square cavity utilizing nanofluids. *International Journal of Heat and Mass Transfer 50*(9), 2002-2018.

Vegad, M., S. Satadia, P. Pradip, P. Chirag and P. Bhargav (2014). Heat transfer characteristics of low Reynolds number flow of nanofluid around a heated circular cylinder. *Procedia Technology 14*, 348-356.

Yang, S. A., R. Y. Hung and Y. Y. Ho (2007). Entropy generation analysis of free convection film condensation on a vertical ellipsoid with variable wall temperature. *World Acad Sci Eng Technol 33*, 189-194.